INHIBITOR STUDIES ON MYCOBACTERIUM TUBERCULOSIS MALATE SYNTHASE

A Senior Honors Thesis

by

JOSHUA L. OWEN

Submitted to the Office of Honors Programs
Texas A&M University
In partial fulfillment of the requirements of the

UNIVERSITY UNDERGRADUATE
RESEARCH FELLOWS

April 2008

Majors: Chemistry and Biochemistry

ABSTRACT

Inhibitor Studies on *Mycobacterium tuberculosis* Malate Synthase

(April 2008)

Joshua L. Owen
Department of Chemistry and
Department of Biochemistry and Biophysics
Texas A&M University

Fellows Advisor: Dr. James C. Sacchettini
Department of Biochemistry and Biophysics and
Department of Chemistry

The emergence of multidrug-resistant strains of *Mycobacterium tuberculosis* (Mtb) has intensified efforts to discover novel drugs for tuberculosis (TB) treatment. Targeting the persistent state of Mtb, a condition in which Mtb is resistant to conventional drug therapies, is of particular interest. Persistent bacteria rely on metabolic pathways that are distinct from active infection Mtb as the environmental conditions of the persistent state are different (e.g., low nutrient). Because persistent Mtb are forced to survive in a low nutrient environment, a short, two enzyme pathway that becomes heavily utilized and upregulated is the glyoxylate shunt. Since the

glyoxylate shunt enzymes are not present in mammals, they make attractive drug targets. We are studying malate synthase (MS), one of the enzymes in the glyoxylate shunt. We used computational, biochemical, and cellular techniques to identify potential inhibitors of MS. Crystal structures of MS in complex with inhibitors were used to rationally design better MS inhibitors. MS inhibitors validated via an enzyme activity assay, were then tested against whole cells using a non-pathogenic form of mycobacteria, *Mycobacterium smegmatis*. In this manner, inhibitors against MS have been identified and characterized for further development into potential novel antitubercular drugs.

DEDICATION

This thesis is dedicated to all of the mentors in my life thus far. They are too vast to name, but they know who they are. I am incapable of expressing the gratitude that is commensurate with their deeds. They have truly been inspiring.

ACKNOWLEDGMENTS

I would like to acknowledge the support of Dr. James C. Sacchettini and the Office of Honors Programs at Texas A&M University.

TABLE OF CONTENTS

LIST OF FIGURES

LIST OF TABLES

CHAPTER I

INTRODUCTION[a]

Tuberculosis (TB) is the leading cause of death worldwide due to an infectious disease, killing around 2 million people annually, primarily in developing countries. Over one-third of the world's population is infected with TB with approximately 8 million new cases of infection every year.[1] TB incidence is also on the rise because of the correspondingly high HIV infection rates. These two diseases progress at faster rates in co-infected individuals.

Mycobacterium tuberculosis (Mtb), the causative agent of tuberculosis, is an obligate aerobe whose sole host is humans. The primary mode of transmission of Mtb is through the air in an aerosolized form, most commonly via a cough or sneeze.[2] Once in the terminal alveoli of the lungs, Mtb is phagocytized by host macrophages. In this early stage of infection, Mtb is able to replicate within non-activated macrophages.[2] However, the body subsequently mounts a cell-mediated immune response to the growing mycobacteria, which includes the activation of macrophages with interferon-γ.[3] The

---

[a] This thesis follows the style and format of *Nature*.

cell-mediated immune response is sufficient 90-95% of the time in controlling the Mtb infection, but not completely eradicating the mycobacteria from the host.[4]

In fact, the remaining mycobacteria will enter into the non-replicating persistence phase or the so called latent stage of the infection. Mtb can reside in alveolar macrophages, avoiding the host immune response for an indefinite period of time. Activation of such latent mycobacteria can occur anytime later in life, especially when the host has become immunocompromised.[2]

Antitubercular drug therapy has existed since the late 1940s,[5] but the long time course of the drug cocktail required for treatment (6-12 months) often causes low patient compliance in completing prescribed regimen. Another problem is the fact that Mtb can survive for extended periods of time in its non-replicative or persistent state. While in this state, Mtb is resistant to conventional forms of chemotherapy. Patient noncompliance coupled with the ability of Mtb to enter the persistence state has contributed to the emergence of multidrug-resistant (MDR) and extensively drug-resistant (XDR) strains of Mtb. The ineffectiveness of current antituberculars against persistent, MDR, and XDR mycobacteria has greatly energized the search for novel anti-TB drugs, including those that target the persistence state.

In order to target the latent stage of the infection, studies have been performed to better understand the extreme intracellular conditions within host macrophages under which dormant Mtb reside. Some of the identified conditions include hypoxia,[6] iron deficiency,[7] low pH,[8] and a fatty acid rich carbon pool[9,10] all contribute to the altered phenotype that Mtb displays in the dormant state. With the sequencing of the Mtb H37Rv genome,[11] it has become possible to map and assign specific genes to their putative functions. Using microarray technology, genes that are upregulated in response to nutrient starvation[12] and latency-like conditions[13,14,15,16] have been identified. The complete genomic sequence coupled with microarray technology has been critical for the identification of metabolic pathways that are required to support the persistent state in Mtb.[17]

One of the changes that occur once Mtb enters the persistent state is an activation of the glyoxylate shunt within the tricarboxylic acid (TCA) cycle.[18,19] This activation facilitates a metabolic shift to acetyl CoA as the primary carbon source, which is the product of the β-oxidation of fatty acids. The glyoxylate shunt consists of two enzymes, isocitrate lyase (ICL) and malate synthase (MS), which act as a bypass to the two CO_2 producing steps in the TCA cycle, thus conserving carbon (which can be used for

gluconeogenesis) and replenishing TCA cycle intermediates in an anaplerotic fashion. The first enzyme in the glyoxylate shunt, ICL, catalyzes the cleavage of isocitrate to succinate and glyoxylate. In the second step, MS condenses glyoxylate and acetyl CoA to produce malate. Since neither ICL nor MS are present in mammals, they have become attractive targets for novel anti-TB drug design.[20]

In Mtb, the genes encoding both ICL and MS are upregulated in response to macrophage phagocytosis.[21,22] It has been reported that an Mtb *icl* knockout strain was able to establish an acute, but not a persistent infection in mice.[19] Also, antibodies to MS have been discovered in 90% of patients during incipient subclinical tuberculosis.[23] According to Bishai,[24] the random insertion of transposons into the Mtb MS gene (*glcB*, annotated Rv1837c)[11] resulted in a non-viability under normal growth conditions; in contrast, Sassetti[25] determined that Mtb MS is not required for tuberculosis infection in mice using a similar transposon insertion method. However, attempts to knockout Mtb *glcB* have been unsuccessful (J. D. McKinney, personal communication). McKinney and colleagues, using *Mycobacterium smegmatis* (closely related to Mtb, but non-virulent), determined that the double knockout of *glcB* and *gcl* (glyoxylate carboligase, not present in Mtb) produced an *M. smegmatis* strain that was unable to grow on acetate

as the sole carbon source, which mimics the macrophage intracellular environment. Additionally, supplementation of Mtb *glcB* into the double knockout *M. smegmatis* strain compensated the knockout phenotype, thus affording the complemented strain with the ability to survive on acetate as the sole carbon source (J. D. McKinney, personal communication).

Mtb malate synthase is an 80 kDa, 741 amino acid monomer. Several crystal structure complexes (substrate-, inhibitor-, and product-bound) of Mtb MS have been reported,[26,27] providing the atomic level details of the Mtb MS active site as well as the binding modes of MS ligands. Using this structural data, inhibitors can be designed to inhibit the activity of MS by exploiting its defined molecular structure.

To begin drug discovery, a library of compounds resembling the natural ligands of an enzyme is assembled and screened for inhibition of enzyme activity to identify so called "hits." Alternative libraries (often as large as 1-5 million compounds) with a broad diversity of chemotypes are also screened so that a large amount of chemical space can be sampled against the enzyme active site of interest. The classical way to screen the library in the pharmaceutical industry is to perform a high throughput screen (HTS) using a rapid, yet reliable assay to determine potential inhibitors from the library

being used.[28] Two rounds of HTS were performed by the Southern Research Institute (SRI) on Mtb MS (totaling 140,000 compounds). The compounds in the library were then ranked based upon the degree to which they inhibited MS catalytic activity, thus providing a preliminary hit list of potential inhibitors to study further.

Another method used to identify potential inhibitors for drug targets is to screen large libraries of compounds by virtual screening (VS). VS is an *in silico* method of computationally fitting ligands into protein active sites. The docking program will use an algorithm to predict the binding energy and interaction modes of the various ligands in the virtual library, which can then be ranked. There are many docking algorithms that have been developed,[29,30,31,32] but DOCK[33,34] is used for MS because of its history of success with reproducing the ligand binding modes of known crystal structure complexes.[35,36] With the Mtb MS active site, a virtual library of over 4 million compounds was sampled *in silico*.[37] The compounds were then scored based upon electrostatic and van der Waals terms, and the generalized Born/solvent accessible surface (GB/SA) model, which rewards the burying of non-polar molecules but penalizes molecules that carry a formal charge for desolvation.[38] The scored and ranked

list of VS hits provides a second list of potential inhibitors that can be compared and studied further in parallel with the hits from the HTS.

The next step is to validate potential inhibitor hits identified from the HTS and the VS. This will be accomplished via a multifaceted approach: First, the inhibitor will be tested *in vitro* against Mtb MS to determine its potency against the enzyme. Second, compounds that have shown promising inhibition *in vitro* will be assayed for growth inhibition against whole cells (*M. smegmatis*). This assay will also assess the ability of the compound to cross the cell wall of the mycobacteria in order to reach its target (MS) as well as assess the specificity of the inhibitor for MS with both knockout and overexpressing strains. In parallel to whole cell testing, attempts will be made to obtain the three-dimensional structure of the most potent inhibitors in complex with MS by x-ray crystallography.

Information from the *in vitro* assays, whole cell assays, and crystal structure inhibitor complexes will aid in the structure-activity relationship (SAR) modification of validated hit compounds used as a starting point for rational drug design. This is done to help optimize solubility, cell permeability, and favorability of interactions of the compound within the active site, thus producing a more specific and potent inhibitor.

Such an optimized MS inhibitor could then be used as a lead compound to target Mtb in the persistent state.

CHAPTER II

METHODS

Malate synthase expression and purification

MS was previously cloned in an *Escherichia coli* pET-15b expression vector with a N-terminal 6X His tag and a thrombin cleavage site. The MS overexpression plasmid was transformed into BL21(DE3) cells. Large scale cultures were grown in LB media 37 ºC with 50 μg/mL carbenicillin, until an OD_{600} of 0.6-0.8. The cultures were then induced with 0.5 mM IPTG for 15 h at 20 ºC. The *E. coli* containing the MS plasmid cultures were then pelleted by centrifugation and resolubilized in Buffer A containing 20 mM Tris pH 7.5, 100 mM NaCl, 5 mM imidazole with 50 μg/mL PMSF, 20 μg benzamidine, and 50 μg/mL DNase. The cells were subsequently lysed using a French press apparatus; the lysate was then centrifuged and the supernatant was filtered through a 0.45 μm filter prior to its loading onto a Ni^{2+} immobile metal affinity chromatography (IMAC) column. After washing with Buffer A, MS was eluted from the column with a linear gradient from 0-100% of Buffer B (20 mM Tris pH 7.5, 100 mM NaCl, 500 mM imidazole). The elution fractions were subsequently run on an SDS-PAGE gel to

confirm which fractions contained MS (80 kDa). Fractions containing MS were dialyzed against Tris buffer pH 7.5 while being incubated with thrombin (1 unit per 2 mg MS), in order to cleave the MS His tag. After dialysis, the protein is again passed over the Ni^{2+} IMAC column, this time with untagged MS found in the flow-through and the tag along with the of uncleaved fraction of MS being left bound to the IMAC column. MS is then dialyzed again with the same buffer composition as before and concentrated using a 50 kDa molecular weight cut-off 50 mL tube concentrator (Amicon Ultra, Millipore).

Malate synthase inhibition assays

Two assays ("direct" and "coupled") for MS inhibition were utilized; both monitor the co-enzyme A (CoA) released as a product from the chemistry of the MS-mediated reaction. Both assays were carried out using 100 µL overall reaction volumes with MS at 92.5 nM being reacted in 20 mM Tris pH 7.5 and 5 mM $MgCl_2$. All inhibitors (in 100% DMSO) were added such that the final reaction mixture contained 1% DMSO (1 µL of stock inhibitor added to the reaction mixture). Inhibitors were incubated with MS in Tris buffer with $MgCl_2$ for 10 min at room temperature before adding the first

substrate: 1.25 mM glyoxylate for the direct assay or 0.06 mM acetyl CoA for the coupled assay. The reaction was initiated by the addition of the second substrate: 0.625 mM acetyl CoA for direct assay or 1.25 mM glyoxylate for the coupled assay.

The "direct" assay measures the loss in absorbance at $\lambda = 232$ nm due to the conversion of acetyl-CoA to CoA. This reaction was continuously monitored for 2 min using a Cary 100 spectrometer with a 100 μL quartz window black cuvette. Reaction with a 1% DMSO solution instead of inhibitor was taken as the uninhibited control. The percent inhibition was calculated by comparing the slope/min values (representing the enzyme velocity) of an inhibitor trial to the uninhibited control.

The "coupled" assay measures the increase in absorbance at $\lambda = 412$ nm due to the formation of 5,5'-dithiobis-(2-nitrobenzoic acid) (DTNB)-CoA adduct.[39] DTNB is injected with glyoxylate at the reaction starting point. A BMG LABTECH POLARstar OPTIMA plate reader in absorbance mode was used to continuously monitor the reaction for 2 min per well of a Corning 96 well plastic plate. The percent inhibition was calculated in a similar manner as the direct assay.

Mycobacterial growth inhibition assay

M. smegmatis strains obtained from J. D. McKinney and colleagues were used for a mycobacterial growth inhibition assay, also known as whole cell testing. The first *M. smegmatis* clone has had the *M. smegmatis* MS (*glcB*) knocked-out along with glyoxylate carboligase (*gcl*), which is not present in Mtb, in order to create a strain unable to grow on acetate as the sole carbon source (*M. smegmatis* Δ*glcB* Δ*gcl*, the "–MS" strain). The knockout strain was then complemented with Mtb *glcB* by genome insertion. The resulting strain (*M. smegmatis* Δ*glcB* Δ*gcl* + *M. tuberculosis glcB*, the "–MS + TBMS" strain) displayed a compensated phenotype and was able to grow on acetate as the sole carbon source.

For this assay, the *M. smegmatis* cells were grown using two different media. The 7H9 media contained Middlebrook 7H9 medium with 0.2% dextrose as the carbon source, 0.085% NaCl, and 0.05% Tween 80. The M9-acetate media contained 1X M9 salts (Sigma) with 0.5% sodium acetate (pH 7.0) as the carbon source, 0.1 mM $CaCl_2$, and 2 mM $MgSO_4$.

A 3 mL 7H9 starter culture with 1 µL of glycerol stock in a 10 mL culture tube was shaken at 37 °C, reaching an OD_{600} of ~2 after around 36 h for both the –MS and

–MS + TBMS clones. The –MS culture was then diluted to 0.001 OD_{600} into 7H9 media and the –MS + TBMS culture was diluted to the same OD_{600} in M9-acetate media.

The diluted cultures were then plated into sterile 96 well plates in a tissue culture hood. Then 4 µL of inhibitor were added to the wells, leaving the outer wells with diluted culture only. Serial dilutions of inhibitors in 100% DMSO were tested starting from 100 µM to 3.125 µM.

The 96 well plates were stored with a set of damp paper towels in a sealed plastic bag and incubated at 37 °C. After 3 d, the results were documented by photographing the plate. To further confirm the level of growth inhibition by color, 5 µL of Alamar Blue (Biosource) was added to each well. After overnight incubation in the dark at room temperature, another photograph is taken of the plate (blue indicates no cellular growth whereas pink indicates cellular growth). The lowest concentration of inhibitor required to inhibit growth was documented as the MIC.

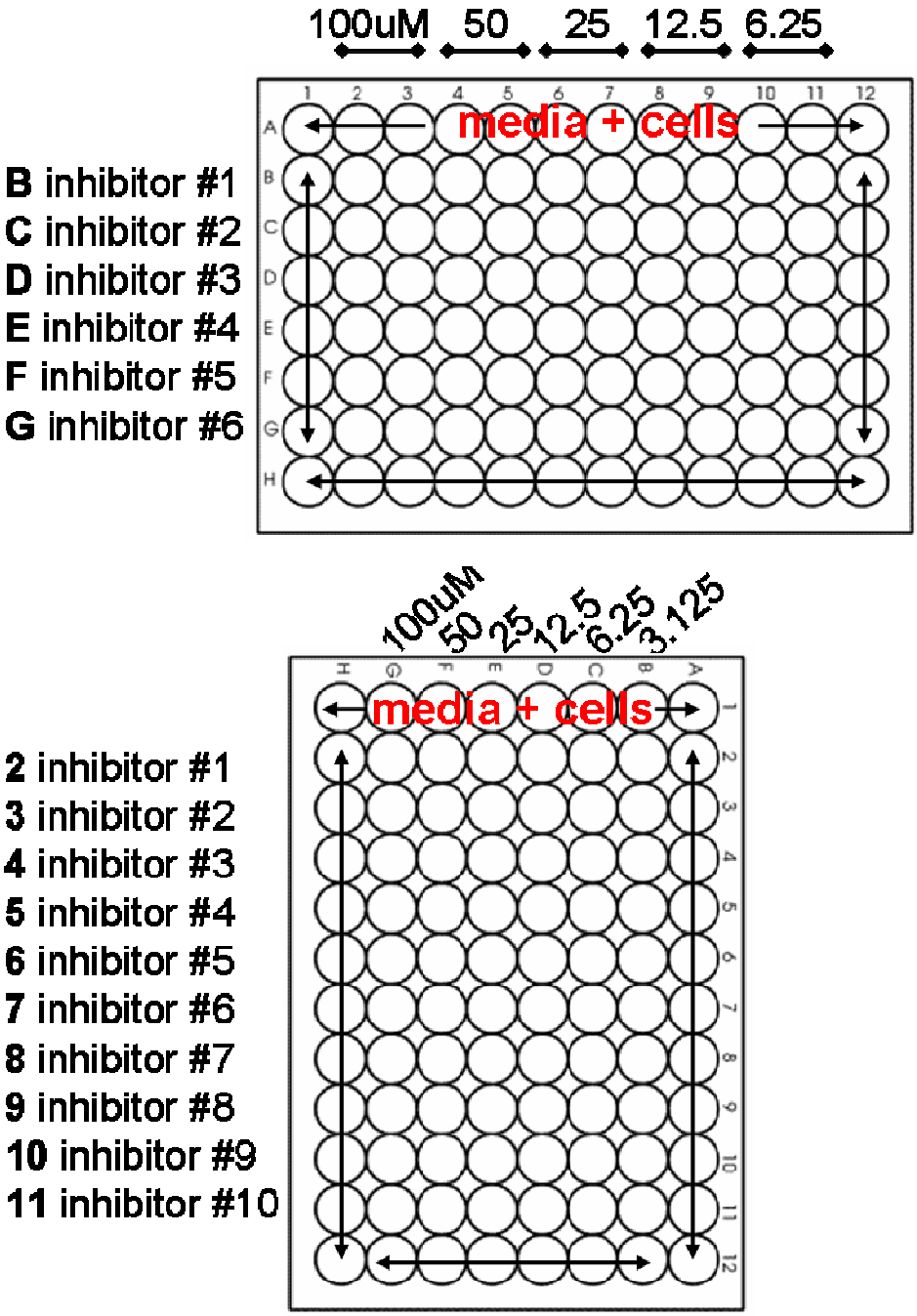

Figure 1. Mycobacterial growth inhibition assay layout. These are two of the most common mycobacterial growth inhibition assay setups. Inhibitors can be set in a variety of ranges and depending on the plate orientation and serial dilution used. The cells only control in the outer wells helps to prevent evaporation in the drug screening wells.

Crystallographic Studies

Crystals of MS were obtained using the hanging-drop vapor diffusion method. The crystallization condition that produced MS crystals contained 100 mM Tris, 100 mM $MgCl_2$, and PEG 3350. Diffraction quality crystals were obtained in pH ranging from 7.5-8.5, PEG from 18-22%, and MS concentrations from 5-8 mg/mL.

As for obtaining MS crystals with a desired inhibitor, co-crystallization and soaking of inhibitors with previously formed MS crystals were attempted. Crystal structures were obtained from crystals soaked with inhibitor starting at a concentration of 2 mM in mother liquor.

MS crystals were harvested using cryo-loops and flash-cooled in liquid nitrogen (using FOMBLIN (Sigma) as a cryoprotectant). Data were collected both on the home radiation source and at the synchrotron at the Advanced Photon Source at Argonne National Laboratory. The home source is an R-axis IV imaging plate system and rotating Cu anode x-ray generator equipped with osmic mirrors. Data were collected over 180°, with 0.5° image widths and 2-4 min of exposure time per frame.

Indexing and scaling was performed using HKL2006.[40] Data were refined via a rigid body refinement in Refmac[41] of the protein chain only of the previously solved Mtb

MS in complex with glyoxylate (PDB #1N8I). Subsequent refinement cycles were performed PHENIX.[42] Modeling and viewing of the MS crystal structures was performed with WinCoot[43] and Chimera[44]. Ligand molecules were built using the eLBOW portion of PHENIX.

CHAPTER III

MOLECULAR VALIDATION AND IDENTIFICATION OF MALATE SYNTHASE INHIBITORS

Malate synthase inhibitor families

Malate synthase (MS) inhibitor identification occurred through the various methods previously mentioned: substrate analog screening, high-throughput screening (HTS), and virtual screening (VS). As MS inhibitors were identified, it was evident that the binding pocket of MS selected for a distinct set of chemotypes. These chemotypes were grouped into inhibitor families. Their molecular identification and study will be described throughout the remainder of this chapter. However, at the time of publication, much of the following is proprietary. Therefore compound structures have been omitted in the text, tables, and figures; the compounds will instead be referred to by an assigned chemical identification number.

PKBA family

Identification

The progenitor inhibitor from the PKBA family was originally identified from a GlaxoSmithKline screen that tested all molecules within their chemical libraries that were similar in structure to reactants, products, or putative transition state compounds of MS. PKBA, standing for phenyl keto butanoic acid, is a phenyl diketo acid that was found to inhibit MS in vitro

Validation with malate synthase enzyme inhibition assay

Testing PKBA inhibition of MS using the DTNB-coupled in vitro enzyme assay, it showed 79% inhibition at 50 μM inihibitor concentration and 29% inhibition at 1 μM. Using the direct in vitro enzyme assay, PKBA exhibited 41% inhibition at 1 μM (Table 1).

PKBA SAR

In order to probe the space around PKBA within the MS active site, a structure-activity relationship (SAR) study was performed. This was accomplished by systematically modifying the base PKBA structure by decorating it with various functional and alkyl groups or substituting whole parts of the molecule for another chemical moiety that

would mimic the original group. The compounds were synthesized in collaboration with Dr. Joel Freundlich and Mr. Justin Roberts at Princeton University.

Once the PKBA SAR compounds were synthesized by Freundlich and colleagues, they were assayed using the DTNB-coupled MS enzyme inhibition assay. The results of which are summarized in Table 1.

Table 1. PKBA SAR compounds and their percent inhibition against MS.

Compound ID	% Inhibition @ 50 μM	% Inhibition @ 1 μM
PKBA	79	29; 41 (d)
JSF-1030	100	68
JSF-1031	100	18
JSF-1032	83	23
JSF-1034	22	23
JSF-1038	100	73
JSF-1039	73	5
JSF-1040	100	20
JSF-1041	99	73
JSF-1042	94	34
JSF-1044	97	11
JSF-1043	97	72
JSF-1047	98	10
JSF-1048	98	37
JSF-1049	96	28
JSF-1050	0	-
JSF-1051	0	-
JSF-1053	98	57

JSF-1058	99	72
JSF-1054	12	-
JSF-1055	0	-
JSF-1056	0	-
JSF-1064	30	-
JSF-1065	95	2
JSF-1069	25	-
JSF-1070	22	-
6679187	0	-
JSF-1071	22	-
JSF-1072	63	-
JSF-1076	12	-
JSF-1085	0	-
5238318	0	-
5238319	0	-
JSF-1118	0	-
JSF-1119	0	-
JSF-1091	0	-
JSF-1097	20	-
JSF-1111	0	-
JSF_1112	0	-
5314457	0	-
633739	0	-
510602	0	-
107395	49 at 100 μM	-
P51605	0	-
156548	0	-
JSF-1123	0	-
JSF-1124	0	-
JSF-1125	0	-
JSF-1126	0	-
JSF-1128	96	85
JSF-1130	0	-

JSF-1131	0	-
JSF-1138	0	-
JSF-1139	0	-
JSF-1154	0	-
JSF-1159	25	-
JSF-1165	0	-
JSF-1166	0	-
JSF-1167	88	6
JSF-1171	0	-
JSF-1172	0	-
JSF-1173	48	-
JSF-1174	37	-
JSF-1175	50	-
JSF-1176	28	-
JSF-1178	19	-
JSF-1179	17	-
JSF-1180	13	-
JSF-1181	100	-
JSF-1182	99	-
223875	0	-
420085	0	-
NSC401908	0	-
223595	0	-
11735636	0	-
244162	0	-
245269	0	-
344830	0	-
245269	0	-
74492	0	-
2756602	0	-
569815	0	-

Overall, 81 PKBA derivatives were tested: 22 have shown inhibition at least 50% inhibition at 50 μM and of those, 7 have shown greater than 50% inhibition at 1 μM. Table 2 summarizes the PKBA SAR compounds that showed great activity against MS than the parent PKBA.

Table 2. PKBA SAR compounds with better percent inhibition of MS than PKBA.

Compound ID	% Inhibition @ 50 μM	% Inhibition @ 1 μM
PKBA	79	29
JSF-1030	100	68
JSF-1031	100	18
JSF-1032	83	23
JSF-1038	100	73
JSF-1040	100	20
JSF-1041	99	73
JSF-1042	94	34
JSF-1044	97	11
JSF-1043	97	72
JSF-1047	98	10
JSF-1048	98	37
JSF-1049	96	28
JSF-1053	98	57
JSF-1058	99	72
JSF-1065	95	2
JSF-1128	96	85
JSF-1167	88	6
JSF-1181	100	-
JSF-1182	99	-

These 19 compounds represent a diverse set of modifications to the parent PKBA structure. Some of these include addition of halogens, alkyl groups, and aryl groups to the phenyl ring of PKBA. The array of acceptable substituents around the phenyl rings indicates additional space in the active site of MS around where the phenyl ring binds in order to accommodate these compounds that are bulkier than the parent PKBA at that location. As these modifications increased the activity of the compound against MS, they could be used to further optimize the activity of PKBA as an eventual antitubercular drug.

Enamine family

Identification

The progenitor of the enamine family was identified from the HTS performed by SRI. The parent compound, 6614887, resembles PKBA, but contains an enamine moiety in the middle of the alkyl chain that is linked to a phenyl containing group.

Validation with malate synthase enzyme inhibition assay

Testing 6614887 inhibition of MS using the DTNB-coupled in vitro enzyme assay showed 74% inhibition at 50 μM inhibitor concentration (Table 3).

6614887 SAR

In order to probe the space around 6614887 within the MS active site, an SAR study was performed. This was accomplished using a two-headed approach: 1) by searching chemical databases and 2) by systematically modifying the base 6614887 structure as was done with the PKBA family. Again, the synthesized compounds were produced through a collaboration with Freundlich and colleagues.

The 6614887 SAR compounds were then assayed to determine the percent inhibition using the DTNB-coupled MS enzyme inhibition assay. The results of which are summarized in Table 3.

Table 3. 6614887 SAR compounds and their percent inhibition against MS.

Compound ID	% Inhibition @ 50 μM	% Inhibition @ 1 μM
6614887	74	-
6193555	89	80
6083251	0	-
5238397	78	46
7265904	70	41
6173566	4	-

5238310	0	-
NSC29078	0	-
S425222	0	-
458295	0	-
NSC204798	0	-
NSC87863	0	-
NSC707051	0	-
JSF-1127	25	-
5241933	0	-
5241916	0	-

Overall, 15 derivatives of 6614887 were tested: 3 have shown inhibition greater than 50% inhibition at 50 μM and of those, 1 has shown greater than 50% inhibition at 1 μM. Table 4 summarizes the 6614887 SAR compounds that showed approximately as great or greater activity against MS than the parent 6614887. These 3 compounds represent both slight (an alkyl group changed to a halogen) and significant (addition of a benzooxazinone group) changes to the parent enamine, 6614887. Possible explanations as to why these modifications to 6614887 are effective include that the active site of MS has the sufficient space or flexibility to accommodate these modifications, or that these inhibitors are degrading to something that is structurally similar to the PKBA family (i.e., smaller compounds). Determination of whether either of these possibilities is accurate is currently ongoing.

Table 4. 6614887 SAR compounds with better percent inhibition of MS than 6614887.

Compound ID	% Inhibition @ 50 μM	% Inhibition @ 1 μM
6614887	74	-
6193555	89	80
5238397	78	46
7265904	70	41

Benzooxazinone family

Identification

The progenitor of the benzooxazinone family, 5238397, was identified from a structure similarity search based upon the enamine family and its original compound, 6614887. 5238397 is similar to 6614887 in structure, except that instead of branching from the PKBA alkyl chain with an enamine, 5238297 does so with a benzooxazinone moiety.

Validation with malate synthase enzyme inhibition assay

As was shown in the enamine family (Tables 3 and 4), 5238397 exhibits 79% inhibition of MS at 50 μM and 46% at 10 μM inhibitor concentration.

Benzooxazinone SAR

In order to further explore the potent effects of 5238387, an SAR study was performed. This was again accomplished using the two-headed approach of searching chemical databases and medicinal chemistry synthesis by Freundlich and colleagues.

The 5238397 SAR compounds were then assayed to determine the percent inhibition using the DTNB-coupled MS enzyme inhibition assay. The results of which are summarized in Table 5.

Table 5. 5238397 SAR compounds and their percent inhibition against MS.

Compound ID	% Inhibition @ 50 μM	% Inhibition @ 1 μM
5238397	78	46
JSF-1148	87	61
JSF-1149	78	56
JSF-1155	41	38
JSF-1156	74	32
JSF-1157	8	0
JSF-1158	63	20
JSF-1160	96	8
JSF-1161	0	-
JSF-1162	34	0
JSF-1150	49	14
5787459	34	-
5283998	70	-
5950194	0	-

5951393	95	89
5284534	36	-
6041664	5	-
5264312	61	47
JSF-1177	0	-
JSF-1170	0	-
JSF-1185	0	-
JSF-1186	65	-
JSF-1188	100	-
JSF-1189	91	-

Overall, 23 derivatives of 5238397 were tested: 11 have shown inhibition greater than 50% inhibition at 50 μM and of those, 3 have shown greater than 50% inhibition at 1 μM. Table 6 summarizes the 5238397 SAR compounds that showed as great or greater activity against MS than the parent 5238397. These 11 compounds primarily represent alkyl, aryl, and halogen modifications to the to the phenyl ring of the "PKBA portion" of the molecule. As the benzooxazinone family compounds are bulkier than either the PKBA or enamine families, modifications that increase the size of the benzooxazinone compounds while increasing their activity indicates that either the MS active site is flexible enough to accept such bulky compounds or that the compounds are degrading to something smaller or more PKBA-like. Studies regarding these two possibilities are currently ongoing.

Table 6. 5238397 SAR compounds with better percent inhibition of MS than 5238397.

Compound ID	% Inhibition @ 50 μM	% Inhibition @ 1 μM
5238397	78	46
JSF-1148	87	61
JSF-1149	78	56
JSF-1156	74	32
JSF-1160	96	8
5283998	70	-
5951393	95	89
JSF-1188	100	-
JSF-1189	91	-

Crystal structures of malate synthase in complex with inhibitors

Crystallization of inhibitor complexes

Many different crystallization methods and conditions were originally attempted with MS. Very few conditions were found and only one was reproducible (described in Methods chapter). In hanging drops, MS crystallizes in two forms: a "fast" form that crystallizes in about 2 weeks to give crystals in the $P4_12_12$ space group with two molecules per asymmetric unit and a "slow" form that crystallizes over about 4 weeks to give crystals in the $P4_32_12$ space group with one molecule per asymmetric unit. The fast form diffracted poorly (~4 Å), whereas the slow form diffracted well (~ 2 Å) on the

home radiation source. Therefore the ligand studies were performed on the $P4_32_12$ crystals.

In order to produce MS:inhibitor complex crystals, both co-crystallization and soaking experiments were attempted. Only soaking inhibitors into previously formed MS crystals was successful.

Malate synthase crystal structure in complex with JSF-1040

A MS crystal structure in complex with JSF-1040 was solved; JSF-1040 is the ortho methyl derivative of PKBA. MS crystals were transferred into a fresh drop of JSF-1040 (2 mM in mother liquor) for soaking. The MS crystals were harvested after 24 h by flash freezing in liquid N_2. The data were collected on the home radiation source. The data collection and refinement statistics can be found in Table 7.

The crystals used for the soaking of JSF-1040 were isomorphous to the previously reported MS:glyoxylate structure (PDB # 1N8I), being in the $P4_32_12$ space group and containing one molecule in the asymmetric unit. Therefore the protein chain model from this PDB entry was used for the refinement of the MS:JSF-1040 complex data.

The overall fold of the MS:JSF-1040 structure is very similar to both the unpublished MS:PKBA complex structure and the published glyoxylate bound structure (PDB #1N8I) as the main protein chain does not move (Figure 2).

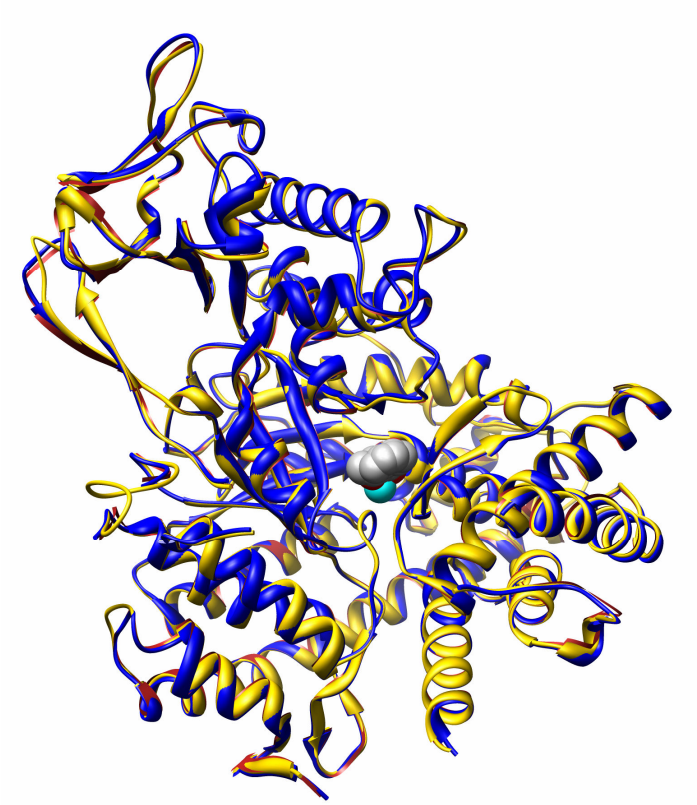

Figure 2. Superposition of MS:ligand complexes. The triple superposition of MS:JSF-1040 (blue), MS:PKBA (yellow), and MS:glyoxylate (red) demonstrates that the overall fold of MS is not altered upon binding of different ligands (shown in space fill).

Similar to PKBA, JSF-1040 was found to bind within the 12 Å long, cylindrical MS active site with its terminal keto group oxygen (2.49 Å) and one of the carboxyl oxygens (2.50 Å) coordinating the Mg^{2+} ion buried at the deep end of the pocket in a bidentate fashion (Figure 3). This bidentate coordination of the Mg^{2+} ion replaces the same coordination of Mg^{2+} by its substrate (or product, malate), glyoxylate (2.08 Å for the carboxylate oxygen and 2.45 Å for the aldehyde oxygen). Thus by completing the octahedral arrangement about the Mg^{2+} ion, JSF-1040 displaces the substrate and thereby competitively inhibits MS. The remaining four coordinations in both the glyoxylate and JSF-1040 complex structures that complete the octahedron around the Mg^{2+} are two conserved water molecules (2.09 and 2.20 Å for glyoxylate and 2.39 and 2.51 Å for JSF-1040 structures), one of the carboxylate oxygens of Glu434 (2.09 Å for glyoxylate and 2.36 Å for JSF-1040 structures), and one of the carboxylate oxygens of Asp462 (2.02 Å for glyoxylate and 2.37 Å for JSF-1040 structures).

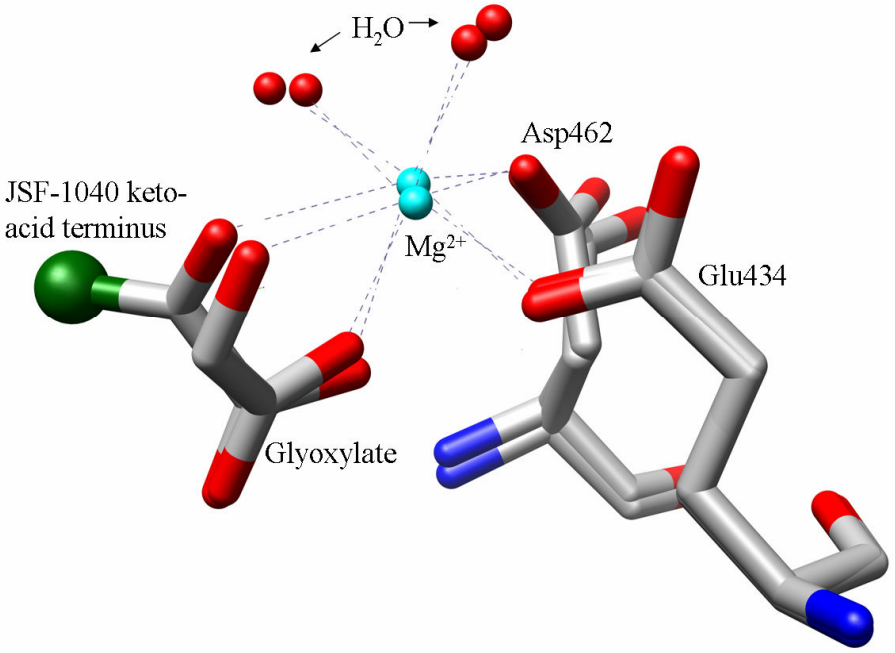

Figure 3. Overlay of magnesium coordination. The MS inhibitor JSF-1040 completes the octahedral coordination of magnesium in the crystal structure, displacing the natural substrate, glyoxylate. The green sphere in this figure represents the remaining part of the JSF-1040 molecule that has been truncated.

JSF-1040 also makes additional contacts and interactions within the MS active site. The two keto groups of JSF-1040 each make a hydrogen bond interaction with the side-chain of Arg339 (2.91 and 3.08 Å). The phenyl ring of JSF-1040 lies in the center of a hydrophobic portion of the MS active site, being surrounded by Val118, Leu461, Met515, Trp541, and Met631. However, these interactions were expected, as they are also found in the MS:PKBA complex structure, with the phenyl ring competing with the

pantothenate moiety of CoA. The ortho methyl group of JSF-1040, its only difference from PKBA, provides some insight into why it has demonstrated a higher percent inhibition of malate synthase activity than PKBA. The ortho methyl group of JSF-1040 projects towards Val118 (3.50 Å), which could serve as a possible hydrophobic interaction partner. This additional hydrophobic interaction may be an indication as to how and where PKBA can be modified to increase its efficacy against Mtb MS.

Malate synthase crystal structure in complex with JSF-1034

A MS crystal structure complex was also solved with JSF-1034; JSF-1034 is the methyl ester of PKBA. MS crystals were transferred into a fresh drop containing JSF-1034 (2 mM in mother liquor) for soaking. The MS crystals were harvested after ~5 d by flash freezing in liquid N_2. The data were collected on the home radiation source. The data collection and refinement statistics can be found in Table 7.

The crystals used for the soaking were isomorphous to the previously reported MS:glyoxylate structure (PDB # 1N8I): they were found to crystallize in the $P4_32_12$ space group with one molecule in the asymmetric unit with the same unit cell dimensions. As with the MS:JSF-1040 complex data, the protein chain from this PDB entry was used for the refinement of the MS:JSF-1034 complex data.

The overall fold of the MS:JSF-1034 structure is the same as the unpublished MS:PKBA structure because the ligand electron density for JSF-1034 reveals the diketo acid PKBA coordinated to Mg^{2+}. Based upon the conditions and the ligand electron density, JSF-1034 (ester of PKBA) most probably hydrolyzed to give the parent PKBA bound to MS.

Malate synthase crystal structures in complex with the enamine and benzooxazinone families

X-ray crystal structures of MS in complex with inhibitors from the enamine and benzooxazinone families have also been attempted in soaking experiments similar to the PKBA family complex structures. However, just like JSF-1034, the inhibitors from the enamine and benzooxazinone families are degraded in the presence of MS and mother liquor to give the corresponding keto acid bound in the MS active site. Further studies to attempt to trap an enamine or a benzooxazinone in the intact form have been unsuccessful thus far.

Table 7. Data collection and refinement statistics for JSF-1040 and JSF-1034 complex structures.

	MS:JSF-1040	MS:JSF-1034
Data collection		
Unit cell (Å)	a = 79.637 b = 79.637 c = 226.156 β = 90.000	a = 79.095 b = 79.095 c = 225.442 β = 90.000
Space group	$P4_32_12$	$P4_32_12$
Number of molecules per asymmetric unit (Z)	1	1
Resolution limit (Å)	46.10-2.80	45.90-2.70
Completeness (%)	96.5 (100.0)	100.0 (99.9)
I/σ	37.9 (14.7)	32.7 (6.5)
R_{sym} [a] (%)	7.3 (21.3)	31.0 (83.1)
Refinement		
Resolution limit (Å)	46.10-2.80	45.90-2.70
Reflections (working/free)	17122/915	19427/1051
R_{work} [b] (%)	17.72	20.22
R_{free} [b] (%)	26.90	29.03
Number of water molecules	523	146
Disordered residues	28	28
Average *B* factor (Å^2) for protein, ligand, and water molecules	38.546, 28.977, 40.012	36.568, 39.330, 36.535
RMS deviations		
Bond length (Å)	0.004	0.006
Angle distances (°)	0.574	0.754

Values in parentheses are for high resolution shells.

[a] $R_{sym} = \sum_h\sum_i |I_{hi} - \langle I_h \rangle| / \sum_h\sum_i I_{hi}$, where I_{hi} is the *i*th observation of the reflection h, whereas $\langle I_h \rangle$ is the mean intensity of reflection h.

[b] $R_{work} = \sum||Fo| - |Fc|| / |Fo|$. R_{free} was calculated with a fraction (5%) of randomly selected reflections excluded from refinement.

CHAPTER IV

WHOLE CELL VALIDATION AND IDENTIFICATION OF MALATE SYNTHASE INHIBITORS

Whole cell assay rationale

The *M. smegmatis* growth inhibition assay, or whole cell assay, was designed to answer a couple questions. First, the ability of a particular inhibitor to cross the cell wall and cell membrane of mycobacteria was assessed. Second, the specificity of a particular inhibitor was assessed by the combination of cell growth inhibition results from the three strains (-MS, -MS + TBMS, and +OE TBMS; see Methods chapter). A specific MS inhibitor should show no inhibition on the –MS strain for two reasons: there is no MS present and 7H9, a full media with dextrose as the carbon source, is the only media on which this strain grows. A specific MS inhibitor should show inhibition on the –MS + TBMS strain on M9-acetate media since MS is present and it is being utilized because acetate is the only carbon source present. Finally, a specific MS inhibitor should show resistance (a higher MIC) on the +OE TBMS strain as the abnormally high intracellular concentrations of MS would compensate the level of inhibition observed.

Growth inhibition studies on the PKBA family

PKBA whole cell activity

One of the obstacles that PKBA presents as a possible antitubercular drug, is that it lacks activity against mycobacteria, beyond the limit of our assay (over 100 μM concentration, Table 8). This is most probably due to the inability of PKBA to cross the cell wall or membrane because of its negatively charged carboxylate. Therefore, part of the rationale behind the PKBA SAR was to not only increase the activity of the PKBA family against the enzyme, but to also impart the family with activity against whole mycobacterial cells (partly by giving them the ability to cross the cell wall or membrane). An example result from the mycobacterial growth inhibition assay is shown in Figure 4.

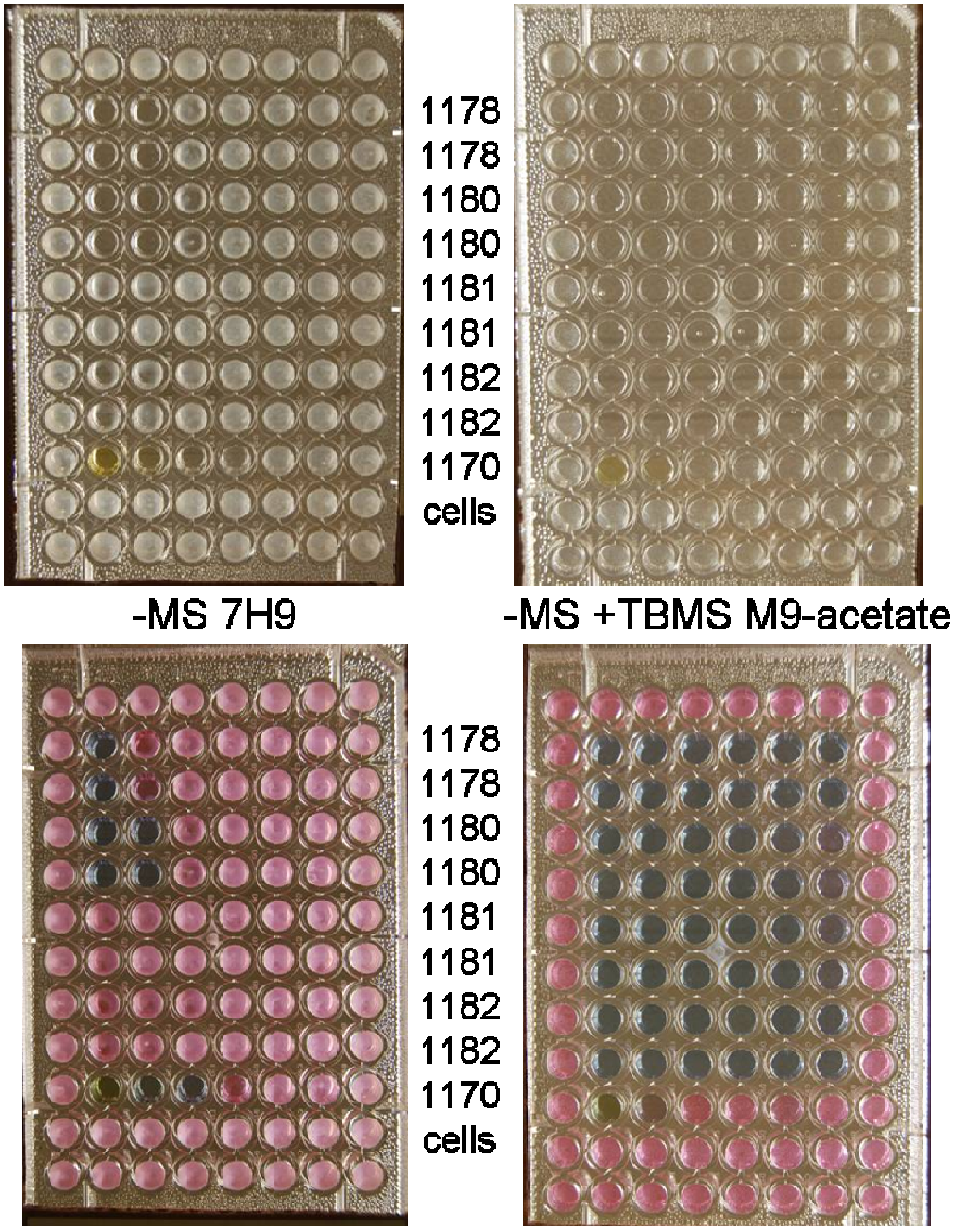

Figure 4. Mycobacterial growth inhibition assay result example. The plates on the left contain the –MS *M. smegmatis* strain in 7H9 media, whereas the plates on the right contain the –MS + TBMS strain in M9-acetate media. Inhibitors are dispensed in rows as shown in Fig. 1. The unstained plates (top plates) represent mycobacterial growth in the presence of inhibitor for 3 days; the Alamar blue stained plates (bottom plates) are on the third day and read on the fourth day (see Methods chapter).

PKBA SAR whole cell activity

The results of the growth inhibition studies with the PKBA SAR compounds are compiled in Table 8.

Table 8. Comparison of PKBA SAR compounds activity against MS and against *M. smegmatis*.

Compound ID	% Inhibition @ 50 μM	MIC (μM) for –MS; -MS + TBMS
PKBA	79	>100; >100
JSF-1030	100	>50; >50
JSF-1031	100	>100; 3.125
JSF-1032	83	>50; >50
JSF-1034	22	>100; >100
JSF-1038	100	>100; 12.5
JSF-1039	73	>100; >100
JSF-1040	100	>100; 0.195
JSF-1041	99	>100; 50
JSF-1042	94	>100; >100
JSF-1044	97	>50; >50
JSF-1043	97	>50; >50
JSF-1047	98	>100; >100
JSF-1048	98	>100; >100
JSF-1049	96	>100; >100
JSF-1050	0	-
JSF-1051	0	-
JSF-1053	98	>100; 50
JSF-1058	99	>100; 25
JSF-1054	12	>100; >100
JSF-1055	0	>100; 100
JSF-1056	0	>100; >100

JSF-1064	30	>100; >100
JSF-1065	95	>50; 3.125
JSF-1069	25	>100; 100
JSF-1070	22	>100; >100
6679187	0	-
JSF-1071	22	>100; >100
JSF-1072	63	>100; 100
JSF-1076	12	>100; >100
JSF-1085	0	>100; >100
5238318	0	>50; >50
5238319	0	>50; >50
JSF-1118	0	>100; >100
JSF-1119	0	>100; >100
JSF-1091	0	>50; >50
JSF-1097	20	50; >100
JSF-1111	0	>100; >100
JSF_1112	0	>100; >100
5314457	0	>50; >50
633739	0	>50; >50
510602	0	>100; >100
107395	49 at 100 μM	-
P51605	0	-
156548	0	-
JSF-1123	0	>100; >100
JSF-1124	0	>100; 100
JSF-1125	0	>100; >100
JSF-1126	0	>100; >100
JSF-1128	96	>100; 100
JSF-1130	0	>100; >100
JSF-1131	0	>100; >100
JSF-1138	0	100; >100
JSF-1139	0	>100; >100
JSF-1154	0	50; 50

JSF-1159	25	>100; 50
JSF-1165	0	100; 100
JSF-1166	0	>100; 6.25
JSF-1167	88	>100; 12.5
JSF-1171	0	100; 12.5
JSF-1172	0	>100; >100
JSF-1173	48	50; 3.125
JSF-1174	37	50; <3.125
JSF-1175	50	25; 50
JSF-1176	28	25; 50
JSF-1178	19	50; <3.125
JSF-1179	17	50; 3.125
JSF-1180	13	25; <3.125
JSF-1181	100	>100; <3.125
JSF-1182	99	>100; <3.126
sig-223875	0	-
420085	0	-
NSC401908	0	-
223595	0	-
11735636	0	-
244162	0	-
245269	0	-
344830	0	-
245269	0	-
74492	0	-
2756602	0	-
569815	0	-

Of the 81 PKBA SAR compounds tested, 17 showed specific inhibition of MS or inhibition on the –MS + TBMS M9-acetate strain only (Table 9). These 17 compounds

represent primarily positional modifications on the phenyl ring of PKBA, including both alkyl groups and halogens. Generally, these observations correlate well with the observations from the enzyme inhibition assays: modifications about the phenyl ring of PKBA, specifically alkyl groups and halogens, are not only tolerated, but also favored against both the enzyme and mycobacterial cells.

Table 9. PKBA SAR compounds exhibiting acetate-specific inhibition of *M. smegmatis*.

Compound ID	% Inhibition @ 50 μM	MIC (μM) for –MS; -MS + TBMS
PKBA	79	>100; >100
JSF-1031	100	>100; 3.125
JSF-1038	100	>100; 12.5
JSF-1040	100	>100; 0.195
JSF-1041	99	>100; 50
JSF-1053	98	>100; 50
JSF-1058	99	>100; 25
JSF-1055	0	>100; 100
JSF-1065	95	>50; 3.125
JSF-1069	25	>100; 100
JSF-1072	63	>100; 100
JSF-1097	20	50; >100
JSF-1124	0	>100; 100
JSF-1128	96	>100; 100
JSF-1138	0	100; >100
JSF-1154	0	50; 50
JSF-1159	25	>100; 50
JSF-1165	0	100; 100

JSF-1166	0	>100; 6.25
JSF-1167	88	>100; 12.5
JSF-1171	0	100; 12.5
JSF-1173	48	50; 3.125
JSF-1174	37	50; <3.125
JSF-1175	50	25; 50
JSF-1176	28	25; 50
JSF-1178	19	50; <3.125
JSF-1179	17	50; 3.125
JSF-1180	13	25; 25
JSF-1181	100	>100; <3.125
JSF-1182	99	>100; <3.126

The ortho position effect

Identification of ortho position effect against mycobacterial cells

One of the most interesting results to arise from the whole cell experiments was an observation about the position effect of substituents on the phenyl ring of PKBA. When the same modification was made to the three different positions on the PKBA phenyl ring (ortho, meta, or para), three different MIC values were observed. Table 10 shows an example of this phenomenon.

Table 10. The position effect of the methyl group on the PKBA phenyl ring.

Compound ID	Modification	% Inhibition @ 50 μM	% Inhibition @ 1 μM	MIC (μM) for –MS; -MS + TBMS
PKBA	-	79	29; 41 (d)	>100; >100
JSF-1040	ortho Me	100	20	>100; 0.195
JSF-1041	meta Me	99	73	>100; 50
JSF-1042	para Me	94	34	>100; >100

As can be seen in Table 10, the position of a methyl group on the phenyl ring of PKBA plays both a factor of the potency of the compound against the enzyme as well as against mycobacterial cells, but a different factor in each case. The ortho (JSF-1040), para (JSF-1042), and meta (JSF-1041) methyl positions, respectively, become increasingly more active against the MS in the coupled assay. However, the ortho, meta, and para methyl positions, respectively, become increasingly worse in activity against mycobacterial cells.

A possible explanation of this effect is the presence of a mycobacterial membrane transporter that specifically recognizes the ortho methyl group in preference to the meta or para methyl group. In order to see if this ortho methyl effect can be extended to other modifications at this ortho position, several other PKBA SAR compounds can be compared (Table 11).

Table 11. The position effect of modifications to the PKBA phenyl ring.

Compound ID	Modification	% Inhibition @ 50 μM	% Inhibition @ 1 μM	MIC (μM) for –MS; -MS + TBMS
PKBA	-	79	29; 41 (d)	>100; >100
JSF-1030	2-naphthyl	100	68	>50; >50
JSF-1031	1-naphthyl	100	18	>100; 3.125
JSF-1032	para-Br	83	23	>50; >50
JSF-1038	ortho-Br	100	73	>100; 12.5
JSF-1043	meta-Br	97	72	>50; >50
JSF-1053	para-Et	98	57	>100; 50
JSF-1058	meta-Et	99	72	>100; 25
JSF-1167	ortho-Et	88	6	>100; 12.5

The data in Table 11 demonstrate that the ortho modification (or "ortho-like" modification in the case of the 1-naphthyl derivative JSF-1031) consistently inhibits growth of mycobacterial cells better than the meta or para position modifications. This is in contrast to the data shown for the enzyme inhibition assay where the meta position is consistently the best (or tied for the best) against the enzyme.

Mycobacterial growth inhibition studies for the enamine and benzooxazinone families are ongoing. These studies include further investigation of the ortho position effect, and whether the probable uptake effect can be seen with the enamine and benzooxazinone families.

CHAPTER V

CONCLUSIONS AND FUTURE DIRECTIONS

The Mtb persistence enzyme, malate synthase, has been studied with various biochemical, computational, and cellular approaches. These studies were initiated because of attractiveness of Mtb MS as a potentially novel antitubercular drug target. Not only is the enzyme MS not found in mammals, but attempts to knockout Mtb MS have been unsuccessful, indicating a possible essential role to Mtb. The discovery of a potent inhibitor against MS would help to validate the essentiality of MS. These studies have identified several inhibitor families upon which further SAR studies have been performed.

The PKBA family SAR has yielded 19 inhibitors for the enzyme assay and 17 inhibitors for the whole cell assay that perform better than the parent PKBA, out of the 81 compounds tested. Similarly, the enamine family SAR has produced 3 inhibitors (out of 15 tested) and the benzooxazinone family SAR has produced 8 inhibitors (out of 22 tested) that exhibit a higher percent inhibition of MS than the parent enamine (6614887) or benzooxazinone (5238397), respectively.

The crystallization and determination of PKBA family inhibitors in complex with MS were successful. JSF-1040 was found to bind in a competitive manner, displacing the substrate glyoxylate, as PKBA does. However, JSF-1040 contains an additional hydrophobic interaction with Val118 via its methyl group at the ortho position on the phenyl ring. JSF-1034 was found to hydrolyze to the parent PKBA and bind in the same orientation as PKBA. The means of hydrolysis (e.g., buffer conditions) of JSF-1034 are currently under study.

Further structural studies are ongoing with the PKBA family and especially the enamine and benzooxazinone families. These studies will help elucidate the possible novel binding modes of the enamine and benzooxazinone family members. These new interactions will be exploited in future SAR and rational drug design studies.

The mycobacterial growth inhibition studies with the PKBA family yielded an interesting result: the position of the modification on the phenyl ring of PKBA effectively fine-tunes the level of inhibition of the compound against *M. smegmatis*. The ortho position on the phenyl ring was found to give exceptionally better MIC values than compared to the meta or para positions.

Studies are currently ongoing for the testing of the enamine and benzooxazinone families in the mycobacterial growth inhibition assay. These results may lead to a better understanding of the effect of a modification at the ortho position of the phenyl ring, including potential explications as to the source of this effect.

The discovery of a potent inhibitor of Mtb MS through biochemical, computational, and cellular approaches would lead to refinement of that hit into a "lead" compound. Lead compounds are then subjected to animal studies as a measure of their toxicity and efficacy. Progress to this stage leaves hope for the development of an antitubercular drug against the persistent Mtb via inhibition of MS.

REFERENCES

1 C. Dye, S. Scheele, P. Dolin et al., *Journal of the American Medical Association* **282**, 677 (1999).

2 J. C. Sherris ed., *Medical Microbiology: An Introduction to Infectious Diseases*, Second ed. (Elsevier, New York, 1990).

3 K. Schroder, P. J. Hertzog, T. Ravasi et al., *Journal of Leukocyte Biology* **75**, 163 (2004).

4 B. R. Bloom and C. J. Murray, *Science* **257**, 1055 (1992).

5 K. Duncan, *Tuberculosis (Edinb)* **83** (1-3), 201 (2003).

6 P. E. James, O. Y. Grinberg, G. Michaels et al., *Journal of Cellular Physiology* **163** (2), 241 (1995).

7 D. Schnappinger, S. Ehrt, M. I. Voskuil et al., *J Exp Med* **198** (5), 693 (2003).

8 Yong-jun Li, Mary Petrofsky, and Luiz E. Bermudez, *Infect. Immun.* **70** (11), 6223 (2002).

9 W. Segal and H. Bloch, *Journal of Bacteriology* **72** (2), 132 (1956).

10 P. R. Wheeler and C. Ratledge, *Journal of General Microbiology* **134**, 2111 (1988).

11 S. T. Cole, R. Brosch, J. Parkhill et al., *Nature* **393** (6685), 537 (1998).

12 J. C. Betts, P. T. Lukey, L. C. Robb et al., *Mol Microbiol* **43** (3), 717 (2002).

13 D. R. Sherman, M. Voskuil, D. Schnappinger et al., *Proc Natl Acad Sci U S A* **98** (13), 7534 (2001).

14 D. G. Muttucumaru, G. Roberts, J. Hinds et al., *Tuberculosis (Edinb)* **84** (3-4), 239 (2004).

15 M. I. Voskuil, K. C. Visconti, and G. K. Schoolnik, *Tuberculosis (Edinb)* **84** (3-4), 218 (2004).

16 H. I. Boshoff, T. G. Myers, B. R. Copp et al., *J Biol Chem* **279** (38), 40174 (2004).

17 G. R. Stewart, B. D. Robertson, and D. B. Young, *Nat Rev Microbiol* **1** (2), 97 (2003).

18 L. G. Wayne and K. Y. Lin, *Infect Immun* **37** (3), 1042 (1982).

19 J. D. McKinney, K. Honer zu Bentrup, E. J. Munoz-Elias et al., *Nature* **406** (6797), 735 (2000).

20 C. V. Smith, V. Sharma, and J. C. Sacchettini, *Tuberculosis (Edinb)* **84** (1-2), 45 (2004).

21 S. Sturgill-Koszycki, P. L. Haddix, and D. G. Russell, *Electrophoresis* **18** (14), 2558 (1997).

22 K. Honer Zu Bentrup, A. Miczak, D. L. Swenson et al., *J Bacteriol* **181** (23), 7161 (1999).

23 K. K. Singh, Y. Dong, J. T. Belisle et al., *Clin Diagn Lab Immunol* **12** (2), 354 (2005).

24 Gyanu Lamichhane, Matteo Zignol, Natalie J. Blades et al., *Proceedings of the National Academy of Sciences* **100** (12), 7213 (2003).

25 C. M. Sassetti and E. J. Rubin, *Proc Natl Acad Sci U S A* **100** (22), 12989 (2003).

26 C. V. Smith, C. C. Huang, A. Miczak et al., *J Biol Chem* **278** (3), 1735 (2003).

27 D. M. Anstrom and S. J. Remington, *Protein Sci* **15** (8), 2002 (2006).

28 D. A. Pereira and J. A. Williams, *Br J Pharmacol* **152** (1), 53 (2007).

29 G. M. Morris, D. S. Goodsell, R. S. Halliday et al., *Journal of Computational Chemistry* **19** (14), 1639 (1998).

30 M. Rarey, B. Kramer, T. Lengauer et al., *Journal of Molecular Biology* **261** (3), 470 (1996).

31 R. Abagyan, M. Totrov, and D. Kuznetsov, *Journal of Computational Chemistry* **15**, 488 (1994).

32 G. Jones, P. Willett, R. C. Glen et al., *Journal of Molecular Biology* **267** (3), 727 (1996).

33 E. C. Meng, B. K. Shoichet, and I. D. Kuntz, *Journal of Computational Chemistry* **12** (4), 505 (1992).

34 D. A. Gschwend and I. D. Kuntz, *Journal of Computer-Aided Molecular Design* **10** (2), 123 (1996).

35 T. J. Ewing and I. D. Kuntz, *Journal of Computational Chemistry* **18**, 1176 (1997).

36 S. Makino and I. D. Kuntz, *Journal of Computational Chemistry* **18** (14), 1812 (1997).

37 J. J. Irwin and B. K. Shoichet, *Journal of Chemical Information and Modeling* **45** (1), 177 (2005).

38 H. Y. Liu, I. D. Kuntz, and X. Zou, *J. Phys. Chem. B* **108** (17), 5453 (2004).

39 George Ellman, *Archives of Biochemistry and Biophysics* **82**, 70 (1959).

40 Z. Otwinowski and W. Minor, *Methods in Enzymology* **276**, 307 (1997).

41 Number 4 Collaborative Computational Project, *Acta Crystallographica Section D - Biological Crystallography* **50**, 760 (1994).

42 P. D. Adams, R. W. Grosse-Kunstleve, L. W. Hung et al., *Acta Crystallographica Section D - Biological Crystallography* **58**, 1948 (2002).

43 P. Emsley and K. Cowtan, *Acta Crystallographica Section D - Biological Crystallography* **60**, 2126 (2004).

44 E. F. Pettersen, T. D. Goddard, C. C. Huang et al., *Journal of Computational Chemistry* **25** (13), 1605 (2004).

JOSHUA L. OWEN

JoshuaLOwen@gmail.com

Education

Texas A&M University, College Station, TX

BS in Chemistry, *BS in Biochemistry, Minor in Philosophy* May 2008

GPA: 4.0/4.0

Research

Department of Biochemistry and Biophysics, Texas A&M University

Texas A&M University Undergraduate Research Fellows Program

Fall 2007-Spring 2008

- Undergraduate thesis in Dr. James C. Sacchettini's lab: *Inhibitor Studies on* Mycobacterium tuberculosis *Malate Synthase*
- Published poster at the American Chemical Society 234th National Meeting in Boston, MA (Aug. 19-23, 2007): *Structure-based Design, Synthesis, and Biological Evaluation of Novel Inhibitors of* Mycobacterium tuberculosis *Malate Synthase*
- Experienced in rational drug design, enzyme assays, whole cell assays, 3D-protein structure determination

Student Researcher in Dr. James Sacchettini's Lab

October 2004-present

- Student Research Week Spring 2005 and 2006: presented a poster on my current research
- Published in *The Journal of Biological Chemistry* [**282**, *37*, 27334-42 (2007)]; helped write and edit text and figures
- Proficient in many lab techniques including preparing buffers, PCR, digestion, ligation, transformation, overexpression, metal-affinity chromatography, crystallization, protein assays, DNA gels, and protein gels

Department of Pharmacology, University of Texas Health Science Center at San Antonio

UTHSCSA Summer Undergraduate Research Program Participant in Dr. Feng Liu's Lab

Summer 2005, 2006

- Oral presentation at the conclusion of each summer, summarizing my research
- Learned many new lab techniques including site-directed mutagenesis, electroporation, transfection, co-immunoprecipitation, confocal microscopy, Western blot, autoradiographic techniques, mammalian cell culture, *Drosophila melanogaster* care and phenotyping

Leadership

Texas A&M Pre-Medical Society

President

Fall 2007-Spring 2008

- Leader of an organization with around 300 members
- Coordinate the activities of the 9 other officers, including scheduling (e.g. physicians to speak at our meetings), community service (e.g. Habitat for Humanity), socials (e.g. medical school field trips)

Secretary

Fall 2006-Spring 2007

- Redesigned and produced the Society newsletter, *The Caduceus*
- Transcribed detailed notes for the Society and disseminated the information to keep everyone informed
- Group Leader for Elder Aid (5 people in group) and The Big Event service projects (15 people in group)

Membership Chair

Fall 2005-Spring 2006

- Maintained the membership points system, collected dues and membership forms, cataloged the members' points so that it was accessible on our website
- Administrator of the listserv (about 700 people), added safety measures to prevent spam e-mails
- Group Leader for Elder Aid and The Big Event community service projects (directed activities of 5 people)
- Designed, organized, and facilitated the painting of a 15' x 4' mural in a food court on campus, completed in 2 weeks

Honors Student Council

Secretary and Webmaster

Fall 2005-Spring 2006

- Redesigned the membership points system, created a new attendance system so that members could keep track of their points
- Overhauled the Council's website; learned rudimentary HTML, CSS, and how to host a website
- Revamped the Honors Course Guide survey that allows honors students to rate their professors

Dean's Student Advisory Panel

Appointed Member

Fall 2005-Spring 2008

- Help recruit future undergraduates and determine College and University level awards for the College of Science

Honors

2008: Chemistry Department Outstanding Undergraduate Award, Chemistry Department Outstanding Analytical Chemistry Student Award, Student Research Week oral presentation first place, Summa Cum Laude, Foundation Honors, University Honors, University Undergraduate Research Fellows

2007: College of Science Dean's Honor Roll, Phi Beta Kappa (inducted), Chemistry Department Achievement Award, Student Research Week poster competition first place

2006: College of Science Dean's Honor Roll, Student Research Week poster competition International Education Week award and second place finisher, Chemistry Department Achievement Award

2005: College of Science Dean's Honor Roll, Outstanding Sophomore Chemistry Award, The Honor Society of Phi Kappa Phi (inducted), Phi Eta Sigma Freshman National Honor Society (inducted)

2004: College of Science Dean's Honor Roll, AP National Scholar